

Parametric study of flow around rectangular prisms using LES

Dahai Yu^{a,*}, Ahsan Kareem^b

^a*Department of Applied Mathematics and Statistics, State University of New York at Stony Brook, NY 11794-3600, USA*

^b*Department of Civil Engineering & Geological Science, University of Notre Dame, Notre Dame, IN 46556, USA*

Abstract

A parametric study concerning the flow around rectangular prisms of different aspect ratios (1:1, 1:1.5, 1:2, 1:3, 1:4) is conducted numerically at a Reynolds number of 10^5 . The Navier–Stokes equations in the large eddy simulation (LES) framework are solved using a finite volume method. The Smagorinsky closure model is used for representing the subgrid scale viscosity. The simulated results clearly demonstrate the influence of the aspect ratio on the velocity field around prisms. Flow reattachment is observed in the mean flow for prisms with aspect ratios of 1:3 and 1:4. This trend in the mean velocity field is corroborated by the mean and RMS distribution of pressure over the prism surface. The numerical results show a good agreement with the available experimental data. © 1998 Elsevier Science Ltd. All rights reserved.

1. Introduction

The geometry of bluff bodies plays a pivotal role in the flow–structure interactions and the resulting flow and pressure fields around them. For rectangular prisms, the separation and reattachment characteristics of the flow are controlled by the prism aspect ratio and the approach flow turbulence. Experimental studies [1–3] involving rectangular prisms have provided important results concerning the pressure distribution on prism faces, lift and drag coefficients and the Strouhal number. The experimental data helps in the validation of numerical simulations. Besides numerical simulation results for square prisms (e.g., Refs. [4–7]), Tamura [8] conducted three-dimensional (3D) simulations of flow around rectangular prisms of various aspect

*Corresponding author. E-mail: dyu@ams.sunysb.edu.

ratios using a direct approach with upwinding as a source of numerical damping. The jump in the Strouhal number at aspect ratios between 2.5 and 3 noted in experimental studies was successfully reproduced numerically [8]. The current work employs a 3D large eddy simulation scheme to study the velocity and pressure field around rectangular prisms. By examining the time-averaged streamline contours and the pressure (mean and RMS values) distributions on the prism surfaces, the current simulation highlights important flow field characteristics.

2. Governing equations and numerical method

The incompressible Navier–Stokes equations recast in the LES format are numerically solved. In this study, the Smagorinsky model is used for the subgrid scale viscosity

$$\frac{\partial \bar{u}_i}{\partial t} + \bar{u}_j \frac{\partial \bar{u}_i}{\partial x_j} = - \frac{\partial \bar{P}}{\partial x_i} + (\nu + \nu_{\text{SGS}}) \frac{\partial \bar{s}_{ij}}{\partial x_j}, \quad (1)$$

$$\frac{\partial \bar{u}_i}{\partial x_i} = 0, \quad (2)$$

$$\nu_{\text{SGS}} = (C_s \Delta)^2 \left[\frac{1}{2} \bar{s}_{ij} \bar{s}_{ij} \right]^{1/2}, \quad (3)$$

and

$$\bar{s}_{ij} = \frac{\partial \bar{u}_i}{\partial x_j} + \frac{\partial \bar{u}_j}{\partial x_i}, \quad (4)$$

where $i, j = 1, 2, 3$, $\Delta = (Dx_1 Dx_2 Dx_3)^{1/3}$ and $C_s = 0.10$ for the 3D computation. For the sake of comparison, selected two-dimensional (2D) computational results are also presented in this paper, in which case, $i, j = 1, 2$, $\Delta = (Dx_1 Dx_2)^{1/2}$ and $C_s = 0.15$. The overbars for quantities in these equations indicate that these quantities are the spatially averaged values used in the LES. These equations are non-dimensionalized using the length of the front side of the rectangular cross section, D , and the inflow velocity, U_0 . The time is nondimensionalized by D/U_0 and pressure with ρU_0^2 , where ρ is the mass density of the fluid. The Reynolds number is thus defined as DU_0/ν , with ν being the fluid kinematic viscosity.

The inflow is specified as the uniform far field flow. On the two lateral side boundaries, either far-field uniform velocity or a free boundary condition, $\partial/\partial n = 0$, can be used. In this study, no significant difference was noted between the results obtained from these boundary conditions. On the spanwise direction, a periodic boundary condition is used. The outflow boundary condition is specified using the Sommerfeld radiation condition, or the convection boundary condition [5–7]. The no-slip and no-penetration boundary conditions are used on the solid walls.

These equations together with the boundary conditions are solved using a finite volume method. The convection terms are discretized with the QUICK scheme, and

the diffusion terms are discretized using the central difference method. The Leith method is employed for temporal marching, and the pressure field is solved with a successive over-relaxation method. Detailed discussions of the numerical methods can be found in Refs. [5–7].

For the numerical simulations reported here, prism front faces are divided into 20 grids of variable size. The smallest grid size ($Dx_{\min} = Dy_{\min} = 0.0416$, $Dz = \text{const} = 0.2$) is used at the corner, whereas the larger grid size is employed near the stagnation line. To eliminate numerical errors, changes in size between two adjacent grids were limited to at most 5%. For the discretization on the lateral faces, the same restriction is used to establish the grids. Away from the prism, the flow domain is discretized in such a manner that the grid size increases as a function of the distance from the prism with similar restriction as noted for the grids on the prism surface. When a prescribed maximum grid size is reached, the grid size in the remaining domain is maintained constant. The total number of grids used for the prisms with aspect ratios of 1.5, 2, 3 and 4 are $220 \times 132 \times 12$, $230 \times 130 \times 12$, $232 \times 132 \times 12$ and $250 \times 130 \times 12$, respectively, and the corresponding domain sizes are $30.35 \times 15.23 \times 2$, $30.35 \times 15.23 \times 2$, $28.78 \times 15.59 \times 2$, and $30.22 \times 15.23 \times 2$. To march for a non-dimensional time of 100 of the flow, about 80 CPU hours of user time are required on an IBM SP2 390 node. A grid refinement study was conducted using a square prism, and the mesh used for the computations reported here correspond to the grid size that has reached convergence. Some of the grid refinement study results are reported in Ref. [7].

3. Numerical simulation results

Numerical simulation results concerning both the velocity and pressure fields are reported in this section. For all the cases reported, the simulated flow Reynolds number is equal to 10^5 . The marching of the numerical simulation starts from an initial potential flow field using a 2D code. The vortex shedding process starts automatically without any artificial disturbance except the round off errors of the computers. After marching for 1000 non-dimensional time units (700 lift force oscillating cycles), the well-developed 2D flow is used as starting flow for a 3D simulation. It then takes about a non-dimensional time of 50 to reach a fully developed 3D flow. When time-averaged values are presented, the first 100 time units are discarded as transient startup flow, and the statistics are conducted over a non-dimensional time length of 500 (about 70 lift force oscillation cycles), or longer when specified.

3.1. Velocity field results

The z -component vorticity contour in the x - y plane are used to visualize the flow field. Fig. 1 shows a sample of instantaneous vorticity contours for prisms with aspect ratios of 1.5, 2, 3 and 4, respectively. In Fig. 1, the x - y plane is sampled at the center of the computation domain, at $K_z = 5$, where K_z is the grid index in the

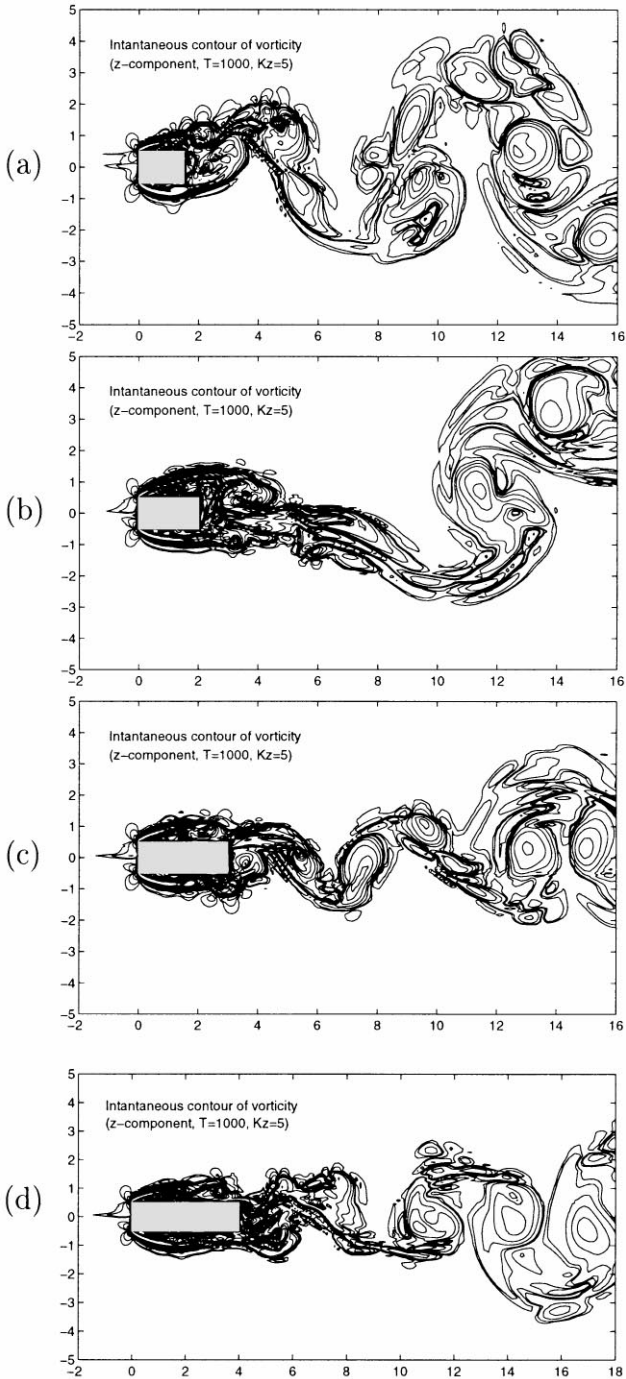


Fig. 1. Instantaneous vorticity contour for rectangular prisms with different aspect ratios: (a) 1:1.5; (b) 1:2; (c) 1:3; and (d) 1:4.

spanwise direction. The fully developed flow field used for this figure is obtained after a non-dimensional time of 1000 from the initial start based on a well-developed 2D flow.

The flow over prism is time-averaged over a period of 500 non-dimensional time units, and the streamlines of the mean flows are presented in Fig. 2. The time-averaged flow is 2D, and also symmetric. The z -component averages out since it is a zero mean process. From Fig. 2, it can be noted that there is a region dominated by reverse flow downstream of the rear face. On the lateral side of the prisms flow separates at the leading corners, and separation bubbles are noted within shear layers. For the flow around prisms of aspect ratios of 1 : 1.5 and 1 : 2, there is no reattachment on the lateral faces similar to the square prism. For the flow around prisms with aspect ratios of 1 : 3 and 1 : 4, the separated flow reattaches to the faces toward the trailing corner. Wind tunnel experiments support these results for smooth inflow conditions. This trend will be further examined in the next subsection using results of the pressure field.

3.2. Pressure field results

Instantaneous pressure contours are plotted in Fig. 3 for the flows around prisms. The plots show pressure contours in an x - y plane at the middle of the computation domain in the spanwise direction. These plots involve the flow field for the results in Fig. 1. The vortex street is obvious from these contours, with staggered low-pressure centers at the core of vortices. It should also be noted that these pressure contours reflect the flow features discernible in the vorticity contours (Fig. 1).

In Fig. 4, the mean pressure distribution around a rectangular prism with an aspect ratio of 1 : 2 is compared with the experimental data from Miyata and Miyazaki [1]. The numerical results with 2D and 3D simulations are in good agreement with the experimental data. For a 1 : 2 rectangular prism, the pressure on the two side faces and the rear face are higher (less negative) than those of a square prism, due to the interaction of the afterbody with the separated flow.

In Fig. 5, the mean pressure distribution on the side faces of prisms with different aspect ratios is presented. The x -axis in the figure is normalized with the prism width. These results demonstrate that with an increase in the streamwise body length, i.e., aspect ratio, there is a concomitant pressure recovery on the side face.

In Fig. 6, the RMS pressure fluctuations on the side face of the rectangular prisms with different aspect ratios are compared. It is noted that a local maximum value of RMS pressure exists for prisms of aspect ratios of 1 : 3 and 1 : 4. This is attributed to the reattachment of the flow to the side face. It can also be noted in Fig. 5 that the mean pressure distribution on the side face of the 1 : 3 rectangular prisms exhibit a pressure increase toward the rear end, while the square and 1 : 1.5 rectangular prisms do not manifest this trend. This suggests reattachment of flow which leads to pressure recovery as the trailing edge of the side face is approached. These results reveal that the 1 : 1.5 rectangular prism, similar to a square, does not exhibit reattachment. The 1 : 2 rectangular prism shows some tendency toward reattachment, while the 1 : 3 and 1 : 4 rectangular prisms indeed experience reattachment.

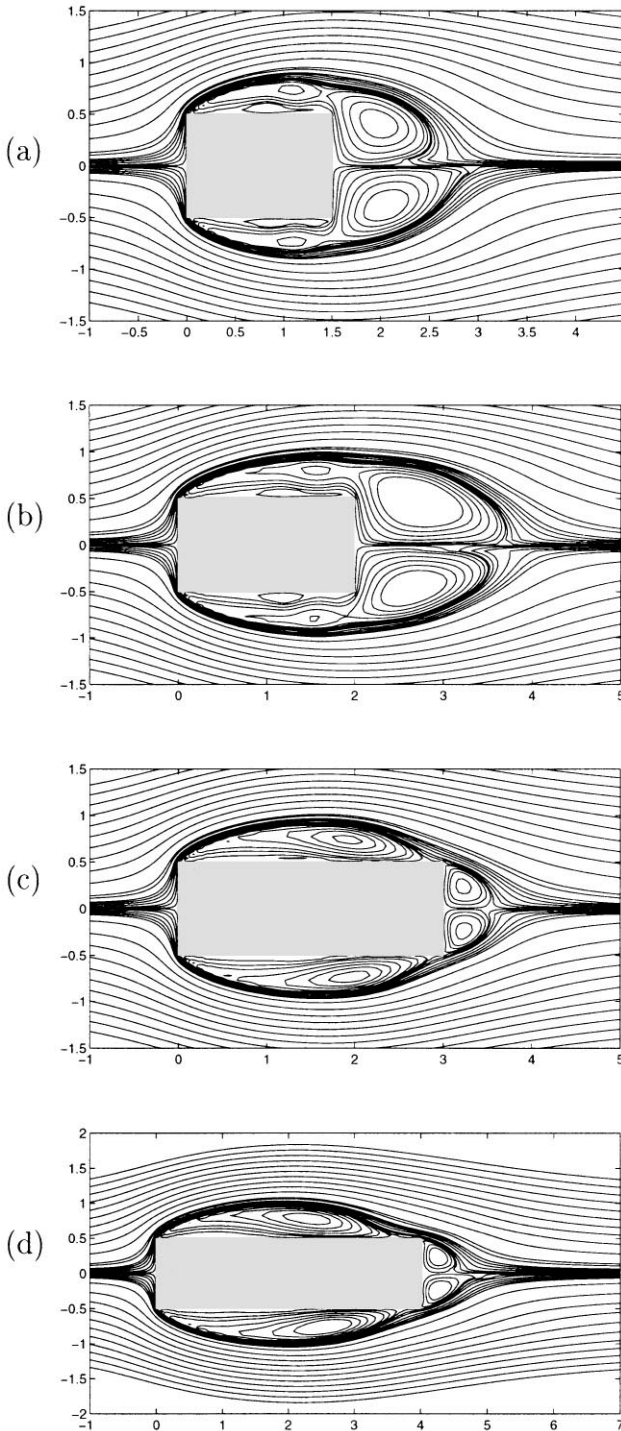


Fig. 2. Streamline of mean flow around rectangular prisms with different aspect ratios: (a) 1 : 1.5; (b) 1 : 2; (c) 1 : 3; and (d) 1 : 4.

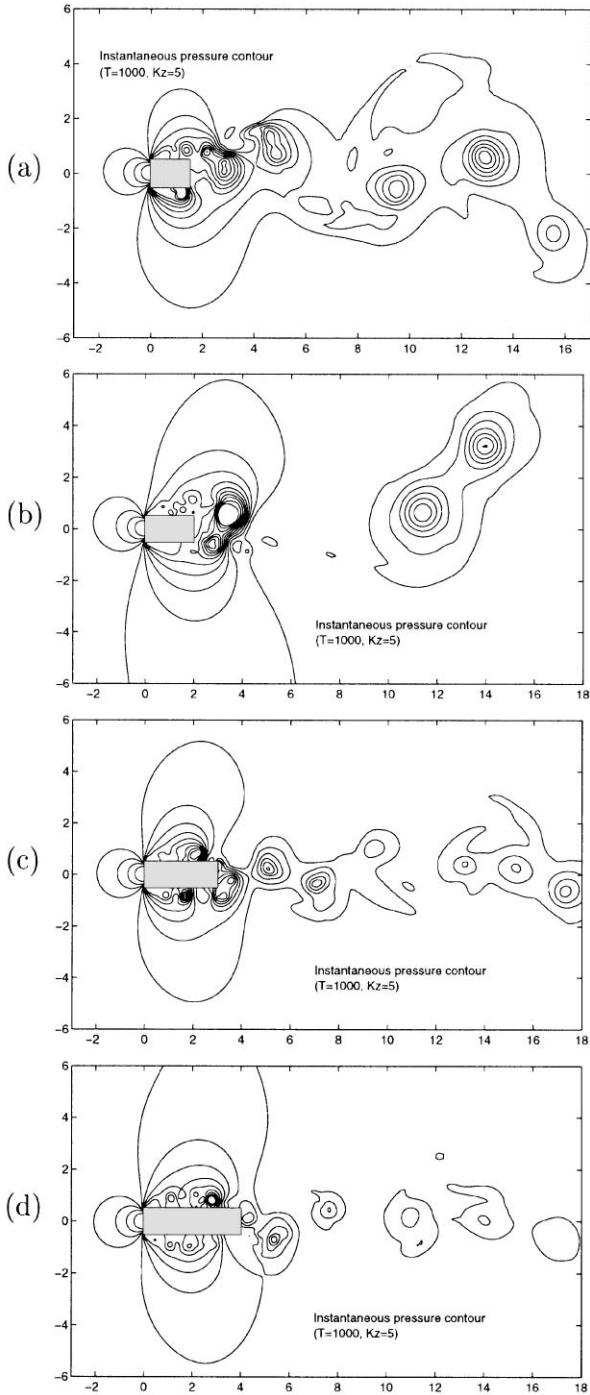


Fig. 3. Instantaneous pressure contours for rectangular prisms with different aspect ratios: (a) 1:1.5; (b) 1:2; (c) 1:3; and (d) 1:4.

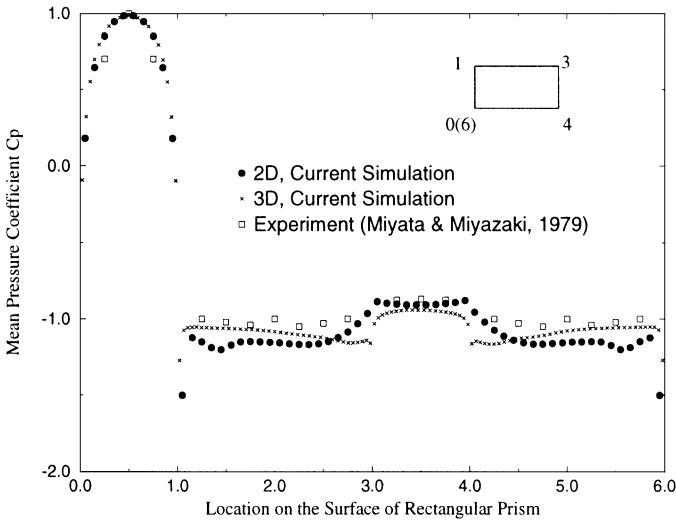


Fig. 4. Mean pressure distribution around a 1 : 2 rectangular prism and comparison with the experimental data.

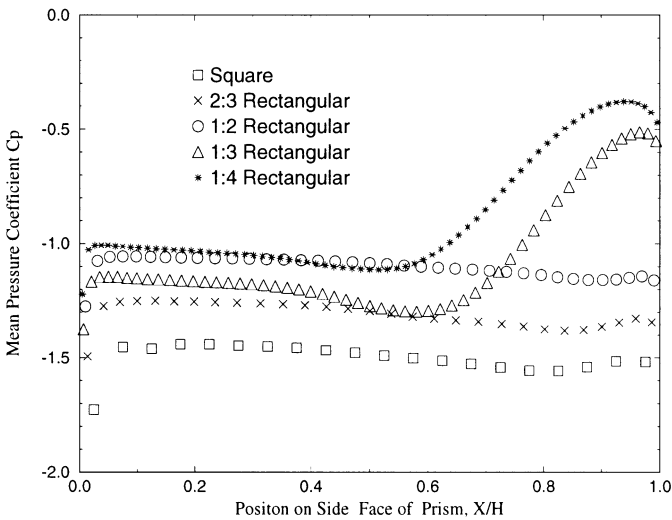


Fig. 5. Comparison of mean pressure distribution on the side of rectangular prisms with different aspect ratios.

Table 1 lists the mean and RMS values of drag force and the Strouhal number for rectangular prisms with aspect ratios from 1 : 1.5 to 1 : 4. Again, it is noted that the mean drag force decreases with an increase in the streamwise length of the body as a result of pressure recovery. This is consistent with the results reported in Fig. 5.

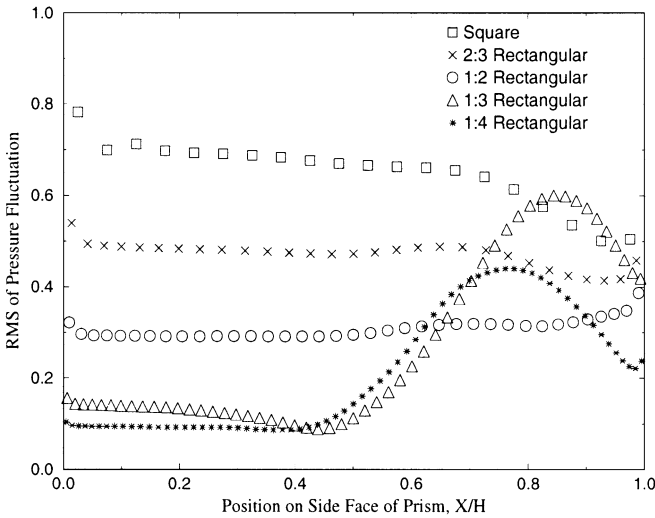


Fig. 6. Comparison of RMS of pressure fluctuations on the side face of rectangular prisms with different aspect ratios.

Table 1
Strouhal number and drag coefficient of rectangular prisms

Aspect ratio ($D:H$)	1:1	1:1.5	1:2	1:3	1:4
Mean of C_D , 2D simulation [5]	2.01	1.72	1.62	1.56	1.43
Mean of C_D , current simulation, 3D	2.14	1.89	1.69	1.3	1.3
Mean of C_D , experiment [9]		1.8	1.6	1.4	1.4
Mean of C_D , experiment [1]			1.65		
Mean of C_D , experiment [10]	2.05				
RMS of C_D , 2D simulation [5]	0.21	0.19	0.14	0.0927	0.168
RMS of C_D , current simulation, 3D	0.25	0.20	0.18	0.14	0.14
RMS of C_D , experiment [10]	0.22				
RMS of C_L , current simulation, 3D	1.15	1.26	1.23	1.03	0.99
RMS of C_L , experiment [10]	1.22				
St, 2D simulation [5]	0.14	0.10	0.18	0.17	0.15
St, current simulation, 3D	0.135	0.107	0.088	0.186	0.156
St, experiment [2]	0.13	0.09	0.08	0.17	0.135

These values are also compared with the available experimental results reported in the literature, and they are generally in good agreement. In comparison with the 2D results, 3D simulation results indicate a significant improvement concerning the Strouhal number for the aspect ratio of 1:2. According to the experiments conducted by Okajima [2], the Strouhal number has a minimum value around the aspect ratio of 1:2, and a maximum at 1:3. This fact is well reproduced in the 3D study, but not in the 2D results.

4. Concluding remarks

A numerical parametric study of the flow around rectangular prisms with different aspect ratios at a Reynolds number 10^5 is conducted using the large eddy simulation method. Based on a grid refinement study, a non-uniform grid mesh is selected for this study. Modifications of the flow caused by the afterbody length are clearly illustrated in both the time-averaged streamline plots and the pressure distribution results. The separation–reattachment characteristics of the flow over the side faces of rectangular prisms are clearly visualized through the mean streamlines. The flow patterns identified by the streamlines are corroborated by the mean and RMS pressure distributions on the side faces. The separated flow reattaches to the side face of prisms with aspect ratios of 1:3 and 1:4. The numerical results of the overall lift and drag forces and Strouhal numbers are found to be in good agreement with the available experimental values.

Acknowledgements

This study was partially supported by NCSA Grant No. BCS960002N, ONR Grant No. 00014-93-1-0761 and NSF Grant No. CMS-9503779.

References

- [1] T. Miyata, M. Miyazaki, Turbulence effects on aerodynamic response of rectangular bluff cylinders, in: J.E. Cermak (Ed.), *Wind Engineering, Proc. Fifth Int. Conf.*, Fort Collins, Colorado, USA, July 1979, pp. 631–642.
- [2] A. Okajima, Strouhal numbers of rectangular cylinders, *J. Fluid Mech.* 123 (1982) 379–398.
- [3] F.A. Da Matha Sant’Anna, A. Laneville, J.Y. Trépanier, Z.Y. Lü, Detailed pressure field measurements for some 2D rectangular cylinders, *J. Wind Eng. Ind. Aerodyn.* 28 (1988) 241–250.
- [4] S. Murakami, A. Mochida, On turbulent vortex shedding flow past 2D square cylinder predicted by CFD, *J. Wind Eng. Ind. Aerodyn.* 54/55 (1995) 191–211.
- [5] D. Yu, A. Kareem, Two-dimensional simulation of flow around rectangular prisms, *J. Wind Eng. Ind. Aerodyn.* 62 (1996) 131–161.
- [6] D. Yu, A. Kareem, Numerical simulation of flow around rectangular prism, *J. Wind Eng. Ind. Aerodyn.* 67/68 (1997) 195–208.
- [7] D. Yu, Numerical simulation of wind-structure interaction, Ph.D. Thesis, Department of Civil Engineering & Geological Science, University of Notre Dame, Notre Dame, Indiana, USA, 1997.
- [8] T. Tamura, Accuracy of the very large computation for aerodynamic forces acting on a stationary or an oscillating cylinder-type structure, IWEF Workshop on CFD for Prediction of Wind Loading on Buildings and Structures, 9 September 1995, Tokyo Institute of Technology, Nagatsuta Campus, Yokohama, Japan, 1995, 2.1–2.22.
- [9] T. Mizota, H. Yamada, Y. Kubo, A. Okajima, C.W. Knisely, H. Shirato, Aerodynamic characteristics of fundamental structures, Part 1, Section 2, *J. Wind Eng.* 36 (1988) 50–52 (in Japanese).
- [10] B.E. Lee, The effect of turbulence on the surface pressure field of a square prism, *J. Fluid Mech.* 69 (1975) 263–282.